Supporting Information

Femto-Microsecond Electron transfer and Intermediates in Al/Fe CO_2 Photoreduction Systems through Optical and X-ray Spectroscopy

Maxime Sauvan[a], Ashok Ugale[a], Lucia Velasco[a,b], Asterios Charisiadis[a], Fan Ma[c], Xiaoyi Zhang[d], Jia-Wei Wang[c*], Dooshaye Moonshiram[a*]

[a.]Instituto de Ciencia de Materiales de Madrid (ICMM-CSIC), Sor Juana Inés de la Cruz, 3, Madrid, 28049, Spain.
[b.]Departamento de Química Física, Universidad Complutense de Madrid, Avenida Complutense s/n, E-28040 Madrid, Spain
[c.]School of Chemical Engineering and Technology, Sun Yat-sen University, Zhuhai 519082, China.
[d]X-ray Science Division, Argonne National Laboratory, 9700 S. Cass Avenue, Lemont IL, 60439, U.S.A

Table of Contents	**Page**

Experimental Section.

X-ray Absorption Spectroscopy (XAS) Methods.

X-ray absorption spectra were collected at the micro-focus undulator B18 beamline at the Diamond Light Source at electron energy 7.1 Kev. The radiation was monochromatized by a Si(111) crystal monochromator. The intensity of the X-rays were monitored by three ion chambers (I_0, I_1 and I_2). I_0, placed before the sample, was filled with 92% nitrogen and 8% argon. I_1 and I_2 were placed after the sample. I_1 was filled with 86 % N_2 and 14 % Ar while I_2 was filled with 100 % Kr. Fe metal was placed between ion chambers I_1 and I_2 and its absorption was recorded with each scan for energy calibration. Fe XAS energy was calibrated by the first maxima in the second derivative of the Fe´s metal foil's X-ray absorption near edge structure (XANES) spectrum. The samples were kept at 15 K in a He atmosphere at ambient pressure and recorded as fluorescence excitation spectra using a 46-element energy-resolving Ge detector. Few mg of the Fe solid catalyst mixed in a 13 mM pellet with Boron Nitride, and 1 mM of the Fe solution complex were measured in a continuous helium flow cryostat in fluorescence mode. Around 10 XAS spectra of each sample were collected. Care was taken to measure at several sample positions on each sample and no more than 5 scans were taken at each sample position. No damage was observed scan after scan to both samples. A beam size 1000 μm(Horizontal) x 1000 μm(Vertical)) was used.

Time-resolved XAS measurements.

Time-resolved X-ray absorption spectra were collected at 11 ID-D beamline[1] at the Advanced Photon Source using the output from an APS standard undulator (3.3 cm period length and a total length of 2.4 m). The experiments were carried out using the 24-bunch timing mode of APS (in top up mode with a constant 102 mA ring current) which consists of a train of X-rays separated by 153 ns.

In this case, the pulse duration of the X-rays is ~78.8 ps (fwhw) at 6.5 MHz delivered from the APS storage ring. The IRF is determined by the laser and X-ray full-width half maximum pulse width. The pulse duration of the laser is very short (1.6 ps) compared to that of the X-ray pulse (~78.8 ps). The IRF is given by equation S1 and is equal to ~78.8 ps.

$$\sqrt{(Laser\ Pulse\ width)^2} + (X-ray\ \ Pulse\ width)^2 \quad \text{(S1)}$$

The separation between two adjacent ~78.8 ps X-ray pulses are long enough for the avalanche Photodiode (APD) detectors to resolve individual X-ray pulses. The complete photocatalytic systems with **Al-1** and **Al-2** with and without BIH were pumped at 400 nm wavelength using a regenerative amplified laser with 10 kHz repetition rate 1.6 ps-FWHM pulse length and laser power of 650 mW. The sample was circulated through a stainless-steel nozzle into a free-flowing 650 μm cylindrical jet inside an airtight aluminum chamber, and continuously degassed with nitrogen. Several batches of ~20 mL were measured and no radiation and laser-

induced damage was observed over the course of 3 hours of time-resolved XANES data collection.

The X-ray and laser beam was spatially overlapped with an X-ray spot size of 100 µm(V) x 450 µm(H) and laser spot size of 170 µm(V) x 750 µm(H). The maximum laser focuses effective area corresponding in this case to the central plane of the cylindrical jet is 170 µm(V) x 650 µm(H). With a liquid flow speed of around 3 m/s, the pumped laser volume was calculated to move out of the FWHM region in around 28 µs. This temporal range ensured that the excited state volume was probed more at the center and less at the edges where the excitation fraction would be less, due to movement of the sample. Beamline 11 ID-D has an automated data digitization system which allows for all X-ray pulses after laser excitation to be collected. Such a system, together with the larger X-ray beam spot size, was very useful for our experiments, as multiple X-ray pulses after laser excitation were averaged to monitor the dynamics for the formation and decay of the photoinduced Fe^{I} transient species in the µs time regime.

The delay between the laser and X-ray pulses was adjusted by a programmable analogy delay line (PDL-100A-20NS, Colby Instruments) and a digital delay line (Highland V851 digital delay/pulse generator). The X-ray fluorescence signals were collected with two APDs positioned at 90˚ on both sides of the liquid jet. Moreover, a combination of Mn Z-1 filters and soller slits with conical geometry were used to reduce the background from elastically scattered X-rays. A Fe metal foil was also placed between two ionization chambers downstream to the X-ray beam, and its transmission recorded with each scan for energy calibration.

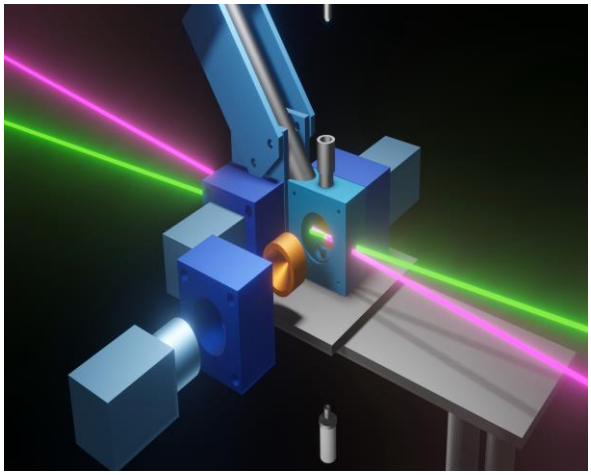

Figure S1. Scheme of the tr-XAS experimental set-up with the spatially overlapped X-ray and laser beams. The sample is being circulated through a stainless-steel nozzle into a free-flowing jet inside an airtight aluminum chamber and the X-ray fluorescence signals are collected with two APDs positioned at 90˚ on both sides of the liquid jet

Optical Transient Absorption Measurements. Ultrafast transient absorption spectroscopy was carried out at the Center for Nanoscale materials at Argonne National Laboratory with an amplified Ti-sapphire laser (Spectra Physics, Spitfire Pro) at 1 KHz repetition rate and an

automated data acquisition system (Ultrafast Systems, Helios). The complexes were pumped with 355 nm excitation and typical pulse energy of 300 nJ per pulse, and probed with a super-continuum (Ultrafast systems, Helios) light source. The transient absorption data included a set of two- dimensional data together with kinetics spectra for a probe wavelength of 460 to 740 nm. The temporal chirp in the optical transient absorption data of the probe beam were corrected using the non-resonant response of blank water, and acetonitrile/DMF solvent, the latter of which gave an IRF of 200 fs. The samples were degassed with N_2 gas and continuously magnetically stirred in a 2 mm cuvette.

Extended X-ray absorption fine structure (EXAFS) analysis.

EXAFS analysis was carried out to determine the near neighbour distances, coordination numbers and atomic species in the Fe-based catalytic complexes. The Athena[2] and Artemis[2] software were used for data processing and analysis respectively. In Athena, the XANES data was first normalized, and the data scaled so that the edge jump is adjusted to 1. The normalization was achieved by subtracting a smooth pre-edge function and post-edge background through a low-order polynomial in ($E-E_0$) where E_0 corresponds to the energy origin or threshold energy. The energy threshold E_0 corresponds to the parameter representing $\mathbf{k}$=0 continuum level at which electrons have just enough energy to propagate through Fe[3] , and was hereby chosen as the energy with the maximum derivative.

The data in energy space was then converted into photoelectron space where $\mathbf{k} = \left[\frac{2m(E-E_0)}{\hbar^2}\right]^{\frac{1}{2}}$. The EXAFS $\chi(\mathbf{k})$ spectrum consisting of a summation of sine waves with amplitudes varying on the atom types and distributions[3] were then weighted by $\mathbf{k}^2$ as the sinusoidal oscillations decrease with increasing $\mathbf{k}$. $\mathbf{K}$-space data were truncated near the zero crossings $\mathbf{k}$ = 2.118 to 13.443 Å^{-1} in Fe EXAFS before Fourier transformation from k to R space. The $\mathbf{k}$-space data were transferred into Artemis Software[2] for the fitting procedure and extraction of the bond distances. The data in fourier transform $\chi(\mathbf{R})$ having separated peaks for various shells were isolated by applying a Hanning window to the first and last 15% of the chosen range. The EXAFS data were subsequently modeled using the EXAFS equation[4] (S2).

$$\chi(\mathbf{k}) = \sum_j \frac{N_j S_0^2 F_i(k)}{\mathbf{k} R_j^2} e^{-2\sigma_j^2 \mathbf{k}^2} e^{\frac{-2R_j}{\lambda_j(\mathbf{k})}} \sin\left(2\mathbf{k}R_j + \delta_j(\mathbf{k})\right) \qquad \text{(S2)}$$

where N_j refers to the average coordination number of atoms in the j^{th} shell; R_j the mean interatomic distance between the Fe (absorbing atom) and the atoms in the j^{th} shell; $F_i(k)$ corresponds to the scattering amplitude and the photoelectron scattering properties of the neighboring atom. The Debye-Waller term $e^{-2\sigma_j^2\mathbf{k}^2}$ corresponds to the degree of disorder due to thermal and structural disorder in absorber-back scatterer distances. The mean free path term $e^{\frac{-2R_j}{\lambda_j(\mathbf{k})}}$ reflects losses due to inelastic scattering, where $\lambda_j(\mathbf{k})$, is the photoelectron mean free path. The oscillations in the EXAFS spectrum are reflected in the sinusoidal term

$\sin\left(2\mathbf{k}R_j + \delta_j(\mathbf{k})\right)$, where $\delta_j(\mathbf{k})$ refers to the phase shift. This sinusoidal term shows the direct relation between the frequency of the EXAFS oscillations in **k**-space and the absorber-back scatterer distance. The amplitude reduction factor, S_0^2, correcting for inelastic effects in the absorbing atom was set to 1 in our EXAFS fitting procedure.

It is important to remark that the number of parameters (N) [3] that can be measured in our data is determined by $\mathbf{N} = \frac{2\Delta k \Delta R}{\pi}$, where $\Delta\mathbf{k}$ and $\Delta\mathbf{R}$ refer to the k and R ranges within which the data are being fitted. The variable parameters that were fitted in this case are elaborated in Table S1 (Supporting information) and correspond to *N*, S_0^2, ΔE_0, *R*, and σ^2 where *N* refers to the number of coordination atoms surrounding Fe for each shell, S_0^2 to the amplitude reduction factor as previously elaborated, ΔE_0 to the change in the threshold energy or edge position, accounting thus for errors in the experimental calibration, *R* to the distance to the neighboring atom and σ^2 to the mean square disorder of the neighboring distance.

The quality of fit was evaluated by R-factor (Equation S3) and the reduced Chi^2 value. The R-factor corresponds to the match between the fit and the data. For instance, the smaller the R-factor, the better is the match between the data and the fit quality.[5] R-factor less than 0.02 denotes that the fit is good whereas R-factor between 0.02 and 0.05 denotes that the fit is correct within a consistently broad model.[5,6] . The reduced Chi^2 value determinations are further employed to compare fits on the same data, as more absorber-backscatter shells are included for the fitting procedure. Similar to the R-factor, a smaller reduced Chi^2 value corresponds to an improved fit.

$$R - factor = \frac{\sum_i (difference\ between\ data\ and\ fit_i)^2}{\sum_i (data)^2} \qquad \text{(S3)}$$

DFT Calculations.

The DFT optimization calculations were performed using the ORCA (Version 5.0) program package developed by Neese[7] and co-workers. Both the ground and excited state geometry optimizations were carried out using the using the BP86[8] as functional with the def2-TZVP[9] triple-zeta basis sets and the D3BJ dispersion correction to account for dispersion corrections respectively. The RI[10] approximation was used to accelerate Coulomb and exchange integrals. The default GRID settings were further used for the self-consistent field iterations and for the final energy evaluation. The CPCM (Conductor-like polarizable model) was also used for the calculations of the solution complexes. The calculated structures were confirmed to be minima based on a check of the energies and the absence of imaginary frequencies from frequency calculations carried out on the optimized geometries.

Time-dependent (TD)-DFT XANES Calculations.

Time-dependent DFT (TD-DFT) calculations for the XANES spectra were performed were carried out using the B3LYP[8, 11] as functional with the def2-TZVP triple-zeta[9] basis sets. The D3BJ [12, 13] dispersion correction was further employed to correct for relativistic effects and

account for dispersion corrections respectively. Up to 150 roots were calculated. A gaussian line shape of 3 eV was applied to all calculated XANES spectra and that of 8 eV was applied to model the time resolved XANES spectra due to the low excited state fraction obtained for the Fe photoreduced species. The donor orbitals for XAS calculations were chosen as Fe 1s and all virtual orbitals were selected as acceptor orbitals. The calculated Fe XANES spectra contain contributions from electric quadrupole, electric dipole and magnetic dipole transitions. A shift of 25.2 eV was applied to all calculated spectra to model the experimental pre-edge and XANES.

Table S1. EXAFS Fits parameters

Sample	**Fit**	**Peak**	**Shell,N**	**R, Å**	**E_0**	**ss.^{2} (10^{-3})**	**R-factor**	**Reduced Chi-square**
Fe solid	1	I	Fe-N, 6	2.15	-0.88	5.7	0.0128	380
Fe solution	1	I	Fe-N, 6	2.13	-4.4	4.1	0.0038	31

*The amplitude reduction factor S_0^2 was set to 1. Peak I refers to the apparent distance between 1.1 -2 Å.

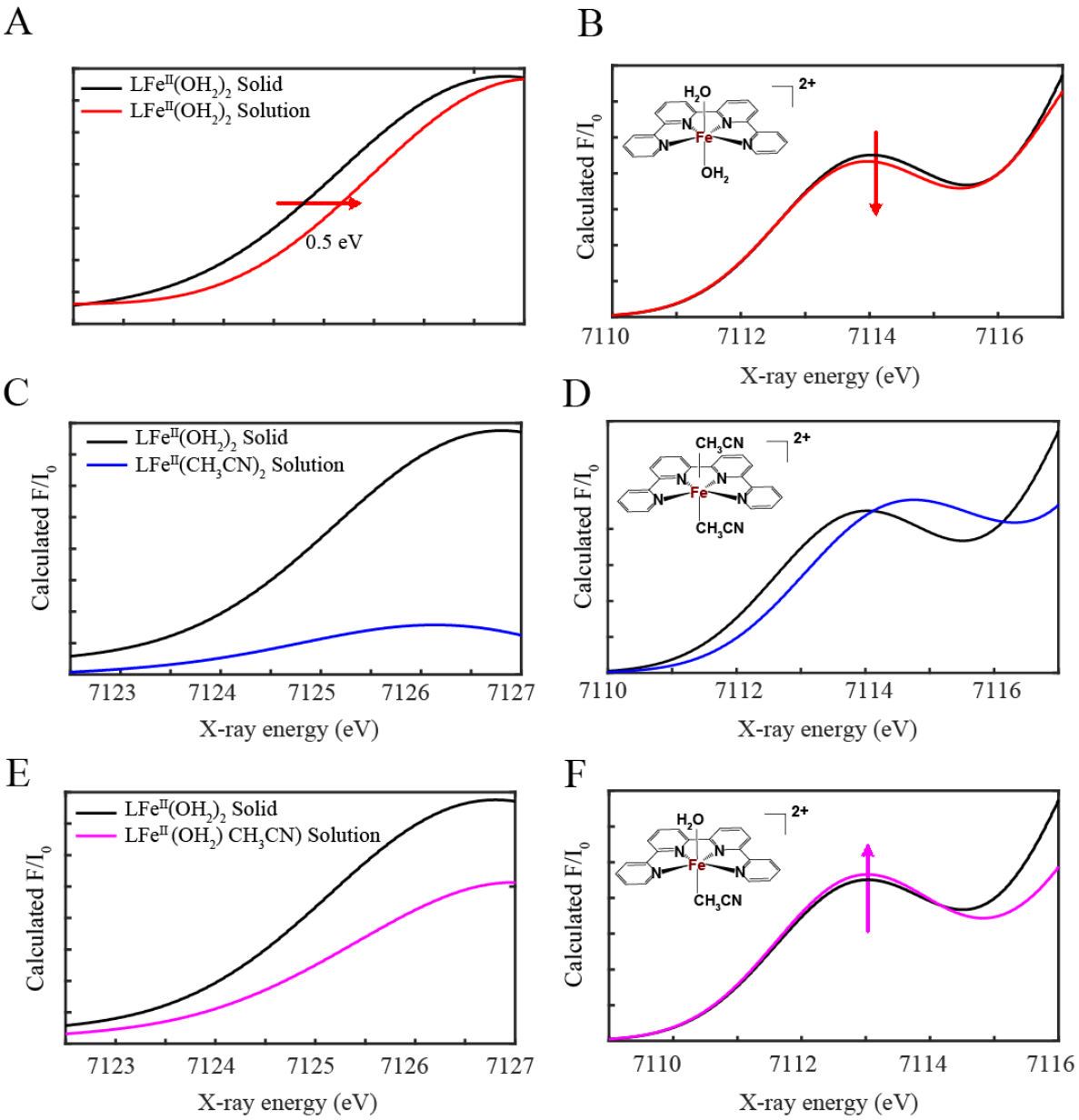

Figure S2. TD-DFT simulated XANES **A.** rising edge and **B.** pre-edge spectra corresponding to the formations of $LFe^{II}(OH)_2$ solid *vs* solution respectively. TD-DFT simulated XANES **C.** rising edge and **D.** pre-edge spectra corresponding to the formations of $LFe^{II}(OH)_2$ solid *vs* $LFe^{II}(CH_3CN)_2$ solution respectively .TD-DFT simulated XANES **E.** rising edge and **F.** pre-edge spectra corresponding to the formations of $LFe^{II}(OH)_2$ solid vs $LFe^{II}(OH_2)(CH_3CN)$ solution respectively.

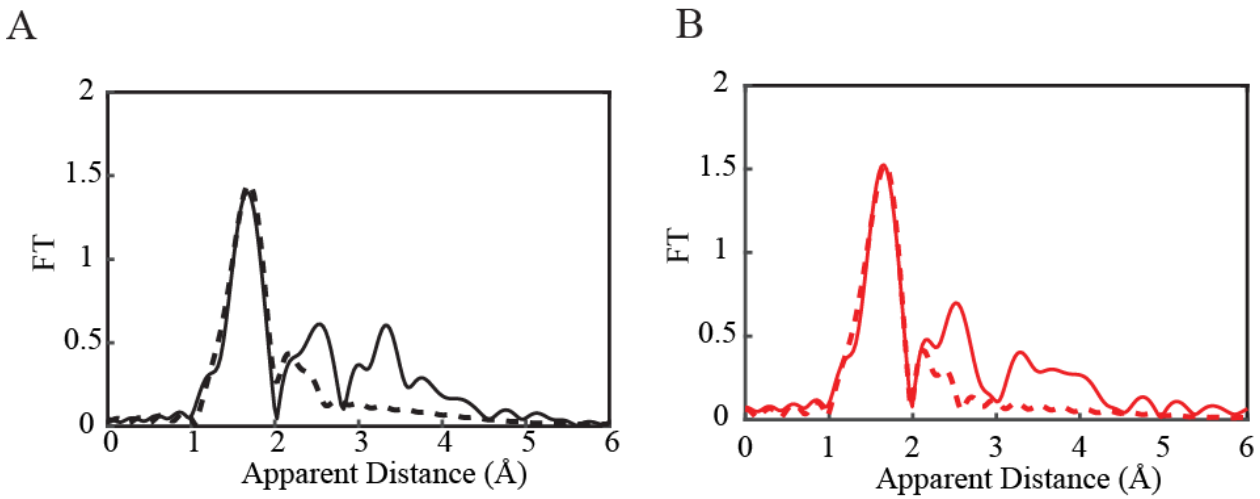

Figure S3: Comparison of the Fourier transform of **A.** Fe catalyst in solid (black) and **B.** solution (red) with their corresponding fits in dashed lines (Table S1).

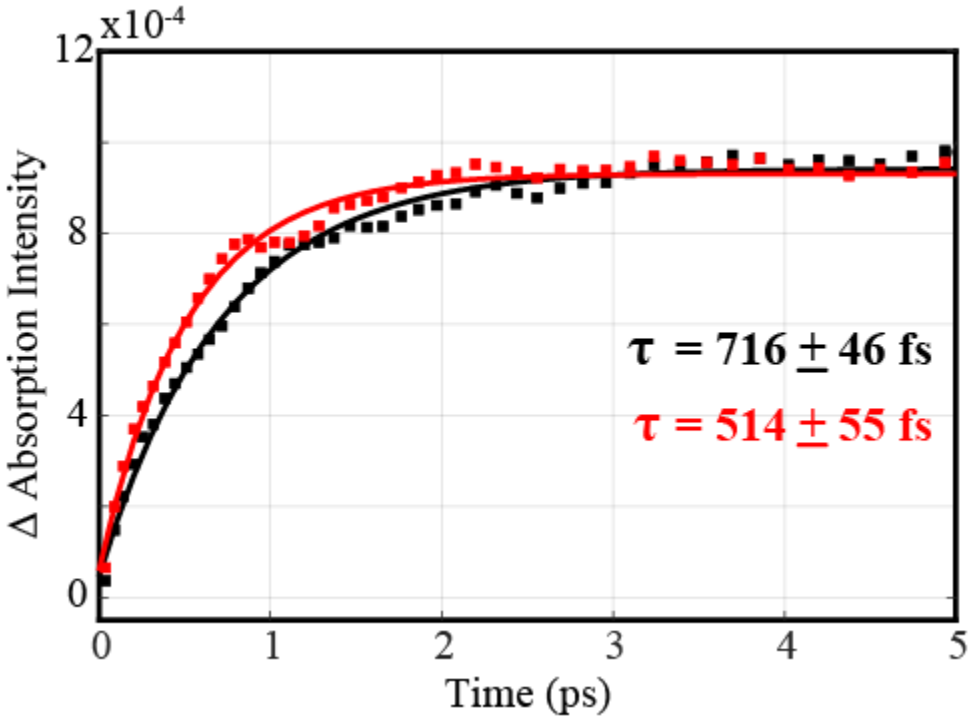

Figure S4: Comparative Kinetic decay profiles at λ = 485 nm after excitation at λ_{exc} = 355 nm illustrating the formation of the **Al*** singlet excited state in **Al-1** (in black) and **Al-2** (in red).

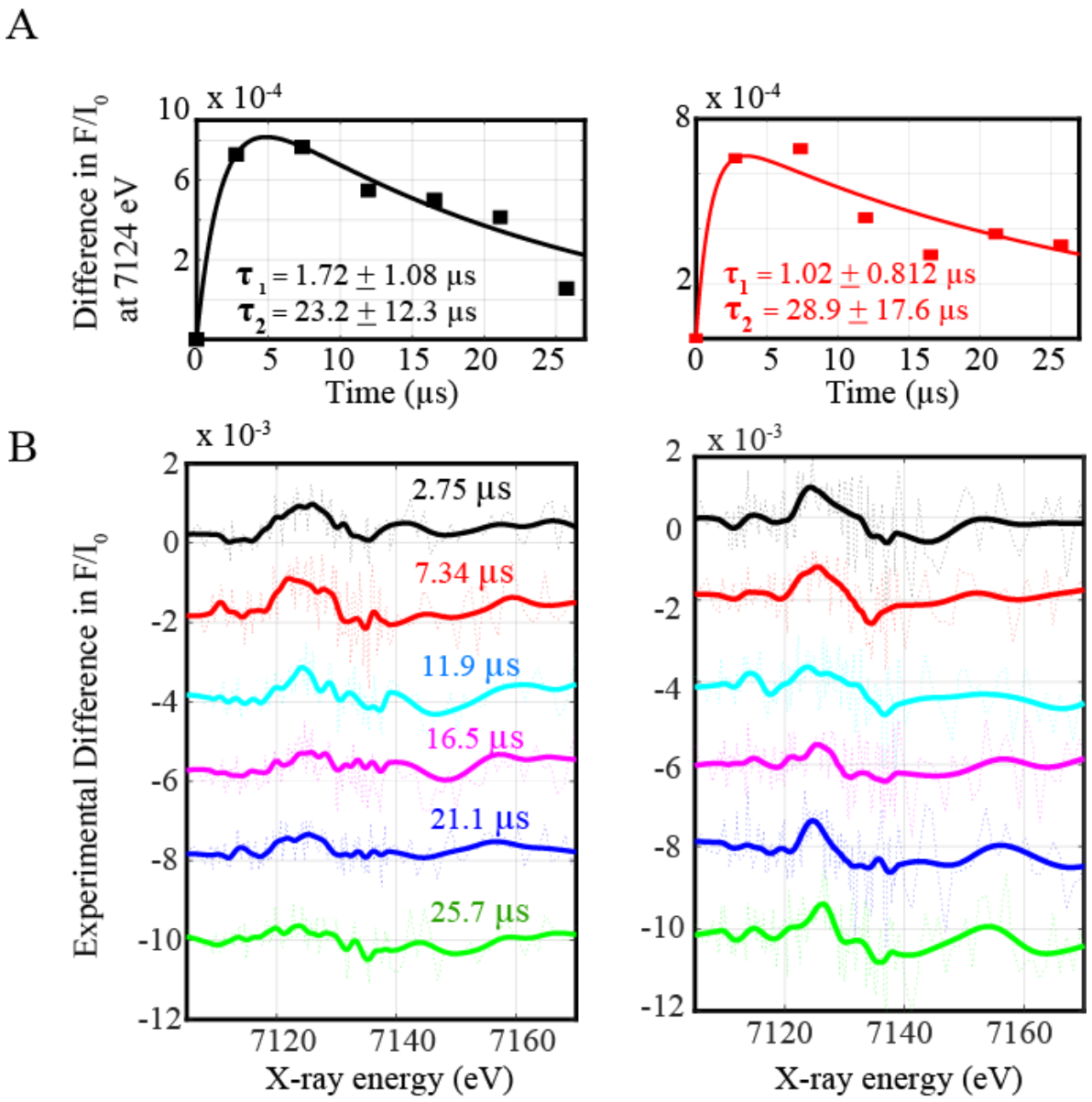

Figure S5 A. Pump-probe time delay scans recorded at 7724 eV for **A. Left.** Multimolecular assembly composed of **Al-1** photosensitizer, Fe catalyst, BIH and TEOA and **Right.** Complete photocatalytic system composed of **Al-2** photosensitizer reflecting the formation and decay of the Fe^{I} photo-induced species. Kinetic fits $\tau_1$and τ_2 of the Fe^{I} formation and decay processes are shown. **B.** Stacked Spectra corresponding to a series of time delays between laser and X-ray pulses. These measurements were carried out for a range of averaged time delays from 2.75 µs to 25.7 µs for the 2 sets of photocatalytic systems with the multimolecular assemblies composed of **Left. Al-1** and **Right. Al-2**

Table S2. DFT calculated parameters of all calculated Fe complexes (Appendix).

Complex	**Fe-N_1**	**Fe-N_2**	**Fe-N_3**	**Fe-N_4**	**Fe-N_5 (CH_3CN)**	**Fe-N_6 (CH_3CN)**	**Fe-OH_1**	**Fe-OH_2**
Fe^{II} solid	2.13848	2.13765	2.12303	2.12338			2.19222	2.19285
	Fe-N_{avg} = 2.151							
Fe^{II} complex with 2 aqua bonds	2.11303	2.11039	2.11126	2.11916			2.17619	2.17582
	Fe-N_{avg} = 2.134							
Fe^{II} complex with 2 acetonitrile molecules	2.18097	2.17843	2.11715	2.11690	2.10025	2.09988		
	Fe-N_{avg} = 2.132							
Fe^{II} complex with 1 acetonitrile molecule and 1 aqua bond	2.13807	2.13071	2.11788	2.12687	2.08552		2.19510	
	Fe-N_{avg} = 2.133							
Fe^{II} complex with 1 aqua bond	2.10427	2.10012	2.08649	2.11303			2.08585	
	Fe-N_{avg} = 2.098							
Fe^{II} complex with 1 acetonitrile molecule	2.11207	2.10985	2.10170	2.10395	1.99885			
	Fe-N_{avg} = 2.085							
Fe^{II} complex with square planar geometry	2.06407	2.06405	2.09282	2.09284				
	Fe-N_{avg} = 2.078							
Fe^{I} complex	2.12003	2.12440	2.06487	2.06019			2.29463	2.28682

with 2 aqua bonds								
	Fe-N_{avg} = 2.158							
Fe^{I} complex with 2 acetonitrile molecules	2.19390	2.19243	2.08359	2.08307	2.08649	2.08727		
	Fe-N_{avg} = 2.121							
Fe^{I} complex with 1 acetonitrile and 1 aqua molecule	2.14905	2.14871	2.07483	2.07336	2.04054		2.33759	
	Fe-N_{avg} = 2.137							
Fe^{I} complex with 1 aqua bond	1.97792	1.97475	1.87735	1.88313			2.28298	
	Fe-N_{avg} = 1.999							
Fe^{I} complex with 1 acetonitrile molecule	1.98199	1.98590	1.89020	1.88878	2.15205			
	Fe-N_{avg} = 1.980							
Fe^{I} complex with square planar geometry	1.97762	1.97756	1.89712	1.89713				
	Fe-N_{avg} = 1.937							

Appendix I- DFT optimized coordinates using the BP-86[8, 11] exchange-correlation functional in combination with the triple zeta valance polarization functions (def2-TZVP)[9] , and the atom-pairwise dispersion correction with the Becke-Johnson damping scheme (D3BJ)[12, 13] in gas phase

Fe^{II} complex with 2 aqua bonds

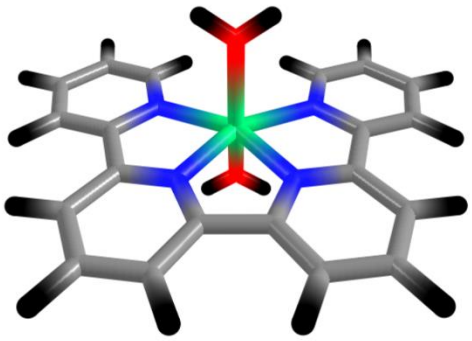

26	14.055178000	0.843792000	3.735876000
7	13.434427000	1.652233000	1.855929000
7	14.681316000	1.649916000	5.614081000
7	13.649014000	-0.854120000	2.527220000
7	14.449248000	-0.855732000	4.945657000
8	16.078021000	1.362217000	3.066588000
8	12.035226000	1.371719000	4.404402000
6	13.346553000	2.969367000	1.586764000
6	13.107425000	0.759498000	0.877407000
6	14.778441000	2.966730000	5.881819000
6	15.002016000	0.755995000	6.593676000
6	13.232201000	-0.660554000	1.261531000
6	13.812723000	-2.094086000	3.033380000
6	14.867277000	-0.663624000	6.211176000
6	14.276654000	-2.094988000	4.440807000
6	12.935824000	3.462934000	0.351188000
6	12.687417000	1.188272000	-0.384717000
6	15.192569000	3.458747000	7.116868000
6	15.424995000	1.183221000	7.855298000
6	12.955905000	-1.755767000	0.430328000
6	13.554185000	-3.223627000	2.256999000
6	15.135645000	-1.759802000	7.043657000
6	14.527011000	-3.225464000	5.218561000
6	12.599934000	2.553506000	-0.653247000
6	15.522043000	2.548110000	8.122326000
6	13.120652000	-3.042130000	0.939476000

6	14.961728000	-3.045534000	6.535893000
1	15.473844000	-1.617632000	8.068192000
1	15.164536000	-3.911821000	7.165397000
1	14.388910000	-4.227570000	4.816284000
1	15.678466000	0.457758000	8.626451000
1	15.850580000	2.895289000	9.101732000
1	15.254023000	4.533616000	7.281671000
1	14.513307000	3.647389000	5.071177000
1	13.616581000	3.649055000	2.396610000
1	12.881868000	4.538025000	0.185207000
1	12.273807000	2.901884000	-1.633033000
1	12.428874000	0.463758000	-1.155073000
1	12.618644000	-1.612312000	-0.594339000
1	12.911591000	-3.907657000	0.310978000
1	13.685092000	-4.226237000	2.660421000
1	16.382790000	1.368877000	2.141826000
1	11.730626000	1.378478000	5.329217000
1	16.873497000	1.365604000	3.628091000
1	11.239686000	1.377876000	3.843019000

Appendix II- DFT optimized coordinates using the BP-86[8, 11] exchange-correlation functional in combination with the triple zeta valance polarization functions (def2-TZVP)[9] , and the atom-pairwise dispersion correction with the Becke-Johnson damping scheme (D3BJ)[12, 13] with the solvent approximation CPCM model.

Fe^{II} complex with 2 aqua bonds

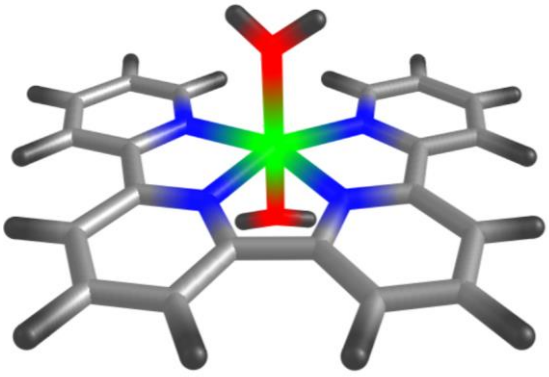

26	14.051400000	0.836033000	3.736828000
7	13.448189000	1.654636000	1.884548000
7	14.662110000	1.654514000	5.583680000
7	13.659659000	-0.857362000	2.524482000
7	14.438283000	-0.852951000	4.943085000
8	16.116167000	1.048828000	3.084415000

8	11.976572000	1.011944000	4.369248000
6	13.369713000	2.974932000	1.636223000
6	13.119539000	0.774212000	0.897508000
6	14.757577000	2.975059000	5.826174000
6	14.990000000	0.773102000	6.570330000
6	13.238073000	-0.650616000	1.266053000
6	13.812622000	-2.094655000	3.032161000
6	14.858457000	-0.649351000	6.203947000
6	14.274436000	-2.092959000	4.441578000
6	12.962629000	3.482673000	0.405154000
6	12.701815000	1.217296000	-0.359545000
6	15.180441000	3.482062000	7.051672000
6	15.422119000	1.216408000	7.823017000
6	12.949001000	-1.739255000	0.430707000
6	13.542063000	-3.220867000	2.254572000
6	15.134479000	-1.738704000	7.043129000
6	14.531654000	-3.218641000	5.223093000
6	12.622005000	2.586471000	-0.609261000
6	15.518862000	2.585054000	8.066875000
6	13.106965000	-3.027086000	0.939046000
6	14.965692000	-3.026511000	6.539808000
1	15.473369000	-1.586096000	8.066053000
1	15.174077000	-3.888264000	7.173588000
1	14.400442000	-4.222490000	4.822815000
1	15.683190000	0.499359000	8.599411000
1	15.856034000	2.946085000	9.038415000
1	15.242623000	4.559363000	7.199268000
1	14.486381000	3.639066000	5.003698000
1	13.642399000	3.639077000	2.458161000
1	12.914840000	4.560146000	0.253427000
1	12.297224000	2.947587000	-1.584955000
1	12.440066000	0.500462000	-1.135848000
1	12.608312000	-1.587624000	-0.591703000
1	12.887957000	-3.888648000	0.308470000
1	13.663392000	-4.224933000	2.657277000
1	16.322257000	1.384513000	2.192468000
1	11.753695000	1.156707000	5.307446000
1	16.782889000	1.433416000	3.682851000
1	11.350681000	1.553216000	3.853404000

Fe^{II} complex with 2 acetonitriles

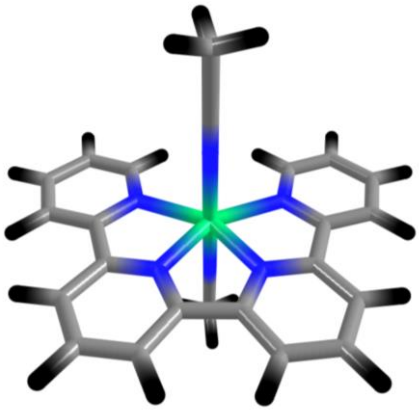

26	14.269320000	1.073378000	3.746030000
7	13.717291000	1.866007000	1.790615000
7	15.038981000	1.877034000	5.618810000
7	13.624011000	-0.603427000	2.626579000
7	14.459935000	-0.597150000	5.032629000
7	12.353635000	1.622995000	4.408681000
6	13.814873000	3.161178000	1.457773000
6	13.268789000	0.967249000	0.879692000
6	15.299796000	3.177072000	5.817995000
6	15.253472000	0.984714000	6.617008000
6	13.203740000	-0.431090000	1.357208000
6	13.624959000	-1.825749000	3.198635000
6	14.928503000	-0.419427000	6.284348000
6	14.116622000	-1.823500000	4.585930000
6	13.469023000	3.631722000	0.192323000
6	12.906594000	1.368283000	-0.409254000
6	15.791657000	3.659331000	7.029585000
6	15.744940000	1.398133000	7.858116000
6	12.753246000	-1.514929000	0.599068000
6	13.186907000	-2.952047000	2.492247000
6	15.074661000	-1.503253000	7.154269000
6	14.238726000	-2.949720000	5.408204000
6	13.008345000	2.715649000	-0.754057000
6	16.016401000	2.750353000	8.064212000
6	12.747633000	-2.785693000	1.180315000
6	14.724033000	-2.778664000	6.703223000
1	15.454927000	-1.363555000	8.164535000
1	14.830895000	-3.638093000	7.364667000
1	13.962823000	-3.938272000	5.045081000
1	15.913910000	0.675696000	8.654692000
1	16.400104000	3.089301000	9.026629000
1	15.990667000	4.723068000	7.151318000
1	15.105465000	3.845178000	4.977063000
1	14.182140000	3.835304000	2.233549000
1	13.562224000	4.691990000	-0.038271000

1	12.729799000	3.045119000	-1.755162000
1	12.551833000	0.640557000	-1.137096000
1	12.410437000	-1.377498000	-0.424638000
1	12.399220000	-3.644759000	0.607499000
6	11.293555000	1.913186000	4.779496000
6	9.972884000	2.272806000	5.239353000
1	9.792136000	3.340741000	5.054903000
1	9.220818000	1.677668000	4.702897000
1	9.891712000	2.071785000	6.316724000
1	13.185863000	-3.936606000	2.956680000
7	16.253024000	1.029533000	3.058658000
6	17.345662000	0.981414000	2.672238000
6	18.705161000	0.921771000	2.189317000
1	19.052306000	-0.120773000	2.182056000
1	19.355837000	1.518200000	2.843712000
1	18.749860000	1.327180000	1.168839000

Fe^{II} complex with 1 acetonitrile and 1 aqua bond

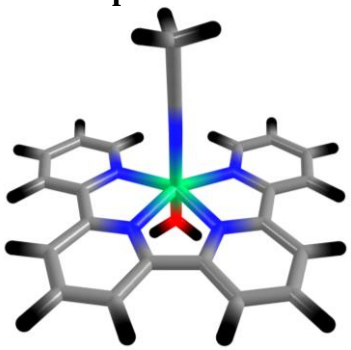

26	14.240830000	1.067990000	3.790707000
7	13.769730000	1.853613000	1.858814000
7	15.037197000	1.862552000	5.600241000
7	13.644501000	-0.623841000	2.648041000
7	14.468672000	-0.615630000	5.055197000
7	12.336164000	1.620007000	4.436404000
6	13.878173000	3.152866000	1.533330000
6	13.308757000	0.973359000	0.929886000
6	15.301369000	3.166463000	5.792781000
6	15.248297000	0.984341000	6.617794000
6	13.229693000	-0.428754000	1.384251000
6	13.633967000	-1.844638000	3.217099000
6	14.926480000	-0.420060000	6.305320000
6	14.121031000	-1.841835000	4.615882000
6	13.534641000	3.639992000	0.274168000
6	12.946918000	1.393501000	-0.352794000
6	15.786316000	3.660524000	7.001035000
6	15.732607000	1.413080000	7.856923000
6	12.769205000	-1.507668000	0.616226000

6	13.189674000	-2.960404000	2.506909000
6	15.058757000	-1.500633000	7.189744000
6	14.226899000	-2.957619000	5.445659000
6	13.060753000	2.742652000	-0.684333000
6	16.004804000	2.765879000	8.050805000
6	12.753772000	-2.776894000	1.190909000
6	14.704346000	-2.773002000	6.747669000
1	15.430023000	-1.352566000	8.202076000
1	14.798358000	-3.627181000	7.417984000
1	13.945618000	-3.948256000	5.092457000
1	15.895226000	0.697622000	8.661236000
1	16.383103000	3.116588000	9.010922000
1	15.986303000	4.725626000	7.109560000
1	15.113451000	3.828436000	4.945605000
1	14.253012000	3.817841000	2.313432000
1	13.640249000	4.702007000	0.056857000
1	12.783005000	3.087333000	-1.680311000
1	12.582944000	0.675719000	-1.086002000
1	12.427930000	-1.361707000	-0.406755000
1	12.398843000	-3.630105000	0.613001000
6	11.260045000	1.890330000	4.775407000
6	9.919690000	2.224896000	5.194994000
1	9.737295000	3.294062000	5.017525000
1	9.194613000	1.635387000	4.616760000
1	9.797113000	2.008575000	6.265150000
1	13.177800000	-3.948687000	2.963043000
8	16.310602000	1.284251000	3.092326000
1	16.511023000	1.017609000	2.175903000
1	17.008226000	0.891262000	3.648886000

Fe^{II} complex with 1 aqua bond

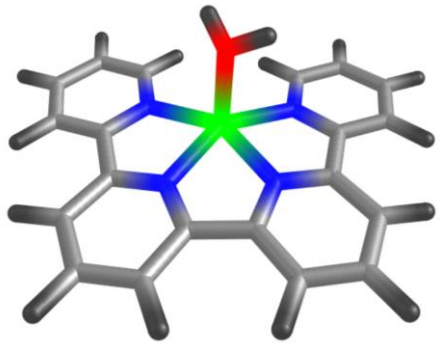

26	13.770753000	0.792320000	3.796300000
7	13.369145000	1.626612000	1.906697000
7	14.674230000	1.643175000	5.490496000
7	13.600581000	-0.881370000	2.517739000

7	14.339839000	-0.866529000	4.926697000
8	11.847408000	1.092901000	4.545405000
6	13.274909000	2.949220000	1.682258000
6	13.103372000	0.759185000	0.890689000
6	14.812170000	2.966880000	5.691529000
6	14.972494000	0.776112000	6.500621000
6	13.232753000	-0.672027000	1.242833000
6	13.771908000	-2.119949000	3.018629000
6	14.812254000	-0.652870000	6.168201000
6	14.212717000	-2.113154000	4.427294000
6	12.911762000	3.471664000	0.442511000
6	12.736834000	1.215950000	-0.374614000
6	15.252133000	3.492946000	6.902652000
6	15.409492000	1.241947000	7.741522000
6	13.012124000	-1.753441000	0.384594000
6	13.561925000	-3.244607000	2.215681000
6	15.132950000	-1.729935000	7.002668000
6	14.517490000	-3.230915000	5.205849000
6	12.638892000	2.589270000	-0.601479000
6	15.549483000	2.613883000	7.944642000
6	13.178954000	-3.046049000	0.888204000
6	14.970163000	-3.026353000	6.511993000
1	15.509001000	-1.565892000	8.010770000
1	15.211597000	-3.880342000	7.144222000
1	14.412343000	-4.237655000	4.804705000
1	15.637025000	0.540238000	8.541833000
1	15.886561000	2.991087000	8.910101000
1	15.349515000	4.571018000	7.020019000
1	14.553150000	3.616539000	4.855069000
1	13.496498000	3.604433000	2.525353000
1	12.847682000	4.550500000	0.309487000
1	12.351598000	2.961907000	-1.584574000
1	12.526231000	0.508587000	-1.174748000
1	12.719763000	-1.598835000	-0.652216000
1	13.011557000	-3.904619000	0.238027000
1	13.697615000	-4.249435000	2.611926000
1	11.754303000	1.035523000	5.516250000
1	11.391201000	1.915743000	4.281320000

Fe^{II} complex with 1 acetonitrile bond

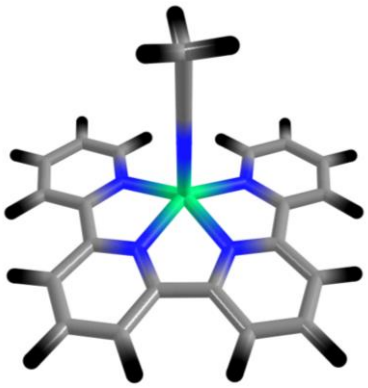

26	13.838218000	1.296363000	3.845998000
7	13.612944000	2.105617000	1.908167000
7	14.921662000	2.108693000	5.463935000
7	13.559783000	-0.385611000	2.613103000
7	14.406192000	-0.380288000	4.978865000
7	11.977819000	1.581876000	4.518889000
6	13.683105000	3.420216000	1.635828000
6	13.213504000	1.239938000	0.935408000
6	15.176104000	3.420598000	5.610728000
6	15.219340000	1.250801000	6.479404000
6	13.196842000	-0.183432000	1.334687000
6	13.653805000	-1.624850000	3.134856000
6	14.931582000	-0.171371000	6.198398000
6	14.143221000	-1.621365000	4.524201000
6	13.362911000	3.938401000	0.382977000
6	12.868803000	1.695198000	-0.337111000
6	15.738197000	3.943812000	6.772902000
6	15.775691000	1.711554000	7.672655000
6	12.868461000	-1.263498000	0.510116000
6	13.339312000	-2.748570000	2.364851000
6	15.181875000	-1.245733000	7.057147000
6	14.370745000	-2.739798000	5.331676000
6	12.945345000	3.059922000	-0.616165000
6	16.037372000	3.073755000	7.820885000
6	12.936171000	-2.553723000	1.043198000
6	14.886095000	-2.537357000	6.612795000
1	15.603881000	-1.086652000	8.047709000
1	15.070934000	-3.390128000	7.265605000
1	14.156657000	-3.744013000	4.969417000
1	16.004330000	1.014357000	8.476902000
1	16.472722000	3.449095000	8.746981000
1	15.931143000	5.012981000	6.845432000
1	14.920438000	4.065879000	4.769929000

1	14.002009000	4.072478000	2.449052000
1	13.439001000	5.010040000	0.205842000
1	12.680352000	3.430528000	-1.606375000
1	12.544297000	0.993707000	-1.103317000
1	12.573632000	-1.111361000	-0.526474000
1	12.684100000	-3.410968000	0.419381000
6	10.897443000	1.755726000	4.904762000
6	9.556057000	1.971138000	5.385035000
1	9.286763000	3.030893000	5.275304000
1	8.855535000	1.351966000	4.807103000
1	9.499410000	1.687240000	6.445667000
1	13.414175000	-3.751213000	2.782569000

Fe^{II} complex with square planar geometry

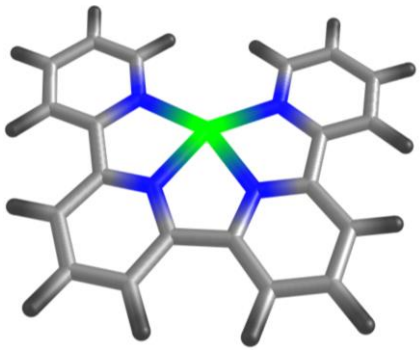

26	14.051995000	0.785991000	3.735852000
7	13.407062000	1.630494000	1.966311000
7	14.696925000	1.630485000	5.505367000
7	13.644630000	-0.886486000	2.545541000
7	14.459366000	-0.886486000	4.926137000
6	13.309278000	2.956908000	1.747795000
6	13.084168000	0.766305000	0.957645000
6	14.794701000	2.956902000	5.723879000
6	15.019822000	0.766296000	6.514036000
6	13.214431000	-0.663216000	1.292692000
6	13.815174000	-2.130149000	3.034888000
6	14.889561000	-0.663222000	6.178988000
6	14.288819000	-2.130150000	4.436793000
6	12.889196000	3.483178000	0.529447000
6	12.658903000	1.232959000	-0.285095000
6	15.214778000	3.483176000	6.942225000
6	15.445082000	1.232958000	7.756774000
6	12.930686000	-1.741031000	0.444083000
6	13.549922000	-3.245586000	2.243288000
6	15.173302000	-1.741040000	7.027599000
6	14.554065000	-3.245588000	5.228392000

6	12.559743000	2.606714000	-0.503462000
6	15.544234000	2.606713000	7.975137000
6	13.104070000	-3.034944000	0.933404000
6	14.999916000	-3.034951000	6.538278000
1	15.520578000	-1.577099000	8.045732000
1	15.214571000	-3.888986000	7.180284000
1	14.419664000	-4.253916000	4.840807000
1	15.697721000	0.528824000	8.547315000
1	15.876225000	2.984802000	8.941805000
1	15.278919000	4.562947000	7.066519000
1	14.531033000	3.612402000	4.894356000
1	13.572946000	3.612413000	2.577315000
1	12.825050000	4.562949000	0.405153000
1	12.227748000	2.984799000	-1.470131000
1	12.406268000	0.528822000	-1.075633000
1	12.583408000	-1.577092000	-0.574050000
1	12.889410000	-3.888977000	0.291398000
1	13.684318000	-4.253915000	2.630872000

Fe^{I} complex with 2 aqua bonds

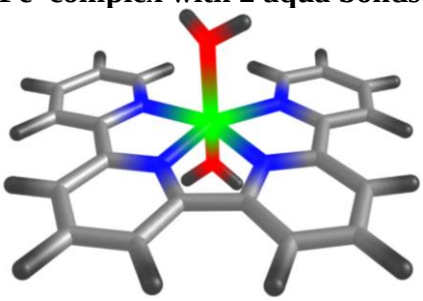

26	14.037197000	0.794787000	3.734707000
7	13.424582000	1.632696000	1.886152000
7	14.619700000	1.629690000	5.599296000
7	13.698205000	-0.842911000	2.531627000
7	14.453314000	-0.842716000	4.921772000
8	16.089724000	1.583744000	3.106816000
8	11.844380000	1.047025000	4.361791000
6	13.351641000	2.956305000	1.628810000
6	13.123434000	0.749372000	0.884861000
6	14.707464000	2.953447000	5.846833000
6	14.984195000	0.750303000	6.581021000
6	13.244940000	-0.661805000	1.260182000
6	13.837786000	-2.104634000	3.035231000
6	14.867078000	-0.661885000	6.206026000
6	14.297038000	-2.104634000	4.424215000
6	12.979478000	3.465942000	0.391538000
6	12.740229000	1.200206000	-0.385535000
6	15.154014000	3.466829000	7.057985000
6	15.442851000	1.203610000	7.825220000

6	12.931544000	-1.751642000	0.443252000
6	13.540375000	-3.227602000	2.260620000
6	15.138153000	-1.750871000	7.038512000
6	14.557832000	-3.227736000	5.212536000
6	12.665795000	2.566093000	-0.637661000
6	15.530794000	2.570423000	8.068451000
6	13.084869000	-3.047490000	0.949972000
6	14.981720000	-3.047149000	6.533303000
1	15.463481000	-1.596144000	8.066357000
1	15.188013000	-3.909975000	7.166234000
1	14.431207000	-4.229849000	4.803746000
1	15.735055000	0.487620000	8.592372000
1	15.891182000	2.935803000	9.030253000
1	15.209358000	4.544977000	7.204232000
1	14.408766000	3.613847000	5.030353000
1	13.604435000	3.619126000	2.458832000
1	12.936271000	4.543656000	0.238299000
1	12.370540000	2.928114000	-1.622618000
1	12.506207000	0.482574000	-1.170790000
1	12.566327000	-1.597900000	-0.571257000
1	12.842401000	-3.910251000	0.329949000
1	13.655201000	-4.229091000	2.674454000
1	16.325281000	1.377994000	2.183211000
1	11.708593000	1.149116000	5.322133000
1	16.797983000	1.185680000	3.645982000
1	11.421722000	1.830512000	3.963496000

Fe^{I} complex with 2 acetonitriles

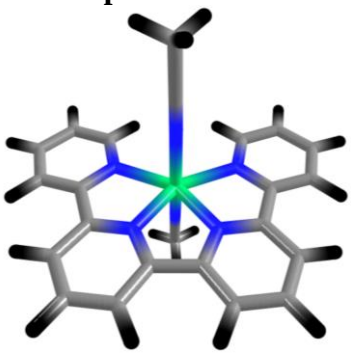

26	14.258689000	0.975749000	3.754401000
7	13.691608000	1.786567000	1.796291000
7	15.047198000	1.787469000	5.632197000
7	13.617410000	-0.663080000	2.639866000
7	14.453115000	-0.661412000	5.028474000
7	12.410451000	1.692178000	4.405694000
6	13.775864000	3.083380000	1.448152000
6	13.242629000	0.884826000	0.880468000
6	15.318023000	3.086749000	5.853033000

6	15.254848000	0.889938000	6.634793000
6	13.187964000	-0.502911000	1.359080000
6	13.617767000	-1.903011000	3.205083000
6	14.926986000	-0.500752000	6.293570000
6	14.108960000	-1.903227000	4.585142000
6	13.423684000	3.551561000	0.186683000
6	12.872355000	1.286323000	-0.411493000
6	15.803976000	3.561769000	7.066542000
6	15.742763000	1.298965000	7.884468000
6	12.741123000	-1.591208000	0.603606000
6	13.181655000	-3.025234000	2.494966000
6	15.072152000	-1.591557000	7.156256000
6	14.233759000	-3.027822000	5.405802000
6	12.962548000	2.629755000	-0.762613000
6	16.020237000	2.644737000	8.103844000
6	12.738599000	-2.865474000	1.179656000
6	14.721095000	-2.867978000	6.705348000
1	15.454698000	-1.452443000	8.166360000
1	14.828176000	-3.730695000	7.362565000
1	13.956682000	-4.014523000	5.036369000
1	15.902146000	0.569324000	8.677341000
1	16.399609000	2.977247000	9.070363000
1	16.007591000	4.624433000	7.194863000
1	15.133646000	3.763733000	5.015752000
1	14.142205000	3.764042000	2.219982000
1	13.509499000	4.612638000	-0.045660000
1	12.678102000	2.956570000	-1.763071000
1	12.518470000	0.552888000	-1.135006000
1	12.397118000	-1.450291000	-0.419882000
1	12.392880000	-3.726046000	0.607350000
6	11.376220000	2.094427000	4.754008000
6	10.087168000	2.588652000	5.188802000
1	10.223394000	3.378638000	5.940514000
1	9.533420000	2.998712000	4.332806000
1	9.505019000	1.769099000	5.633175000
1	13.185296000	-4.009856000	2.961108000
7	16.220026000	1.108371000	3.052780000
6	17.313399000	1.173340000	2.661417000
6	18.675509000	1.247952000	2.177086000
1	19.105428000	0.238061000	2.118580000
1	19.284311000	1.855809000	2.860858000
1	18.693880000	1.703011000	1.177157000

Fe^{I} complex with 1 acetonitrile and 1 aqua bond

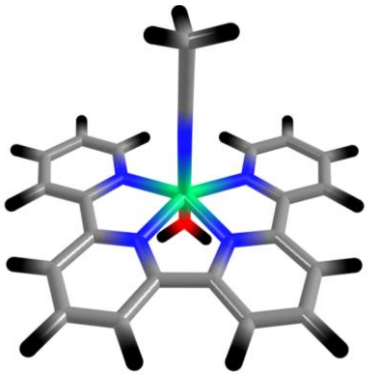

26	14.176212000	1.020743000	3.796564000
7	13.759518000	1.817636000	1.844712000
7	15.015073000	1.829844000	5.601734000
7	13.641289000	-0.626039000	2.656044000
7	14.445950000	-0.618995000	5.038902000
7	12.330179000	1.628631000	4.418216000
6	13.845557000	3.122494000	1.519095000
6	13.302472000	0.933813000	0.910656000
6	15.271716000	3.137441000	5.802039000
6	15.223217000	0.952580000	6.625862000
6	13.246342000	-0.460116000	1.364936000
6	13.647330000	-1.870918000	3.212730000
6	14.910371000	-0.444563000	6.305611000
6	14.114828000	-1.866738000	4.599425000
6	13.487786000	3.613732000	0.268962000
6	12.923142000	1.362748000	-0.368816000
6	15.742170000	3.637860000	7.010449000
6	15.694679000	1.390738000	7.871062000
6	12.833129000	-1.547142000	0.589437000
6	13.241596000	-2.991628000	2.483225000
6	15.052698000	-1.526388000	7.179273000
6	14.234010000	-2.982354000	5.432504000
6	13.015683000	2.712107000	-0.694878000
6	15.957645000	2.742732000	8.067481000
6	12.829329000	-2.825599000	1.158070000
6	14.707794000	-2.807897000	6.735886000
1	15.427309000	-1.377032000	8.190991000
1	14.809953000	-3.664153000	7.402261000
1	13.962341000	-3.973504000	5.070646000
1	15.852675000	0.676397000	8.678107000
1	16.324903000	3.097282000	9.030748000
1	15.935884000	4.704383000	7.119834000
1	15.088539000	3.797167000	4.951378000
1	14.217666000	3.787888000	2.300876000
1	13.578061000	4.678355000	0.055897000
1	12.723588000	3.059516000	-1.686068000

1	12.557376000	0.644159000	-1.101167000
1	12.519144000	-1.403966000	-0.443490000
1	12.509177000	-3.685854000	0.570604000
6	11.283361000	1.972717000	4.792827000
6	9.981727000	2.398593000	5.260115000
1	9.858992000	3.477391000	5.089043000
1	9.193199000	1.859476000	4.716356000
1	9.881537000	2.193370000	6.335196000
1	13.246974000	-3.980427000	2.940741000
8	16.360874000	1.437928000	3.077149000
1	16.520190000	1.072676000	2.187447000
1	16.984841000	0.967800000	3.660048000

Fe^{I} complex with 1 aqua bond

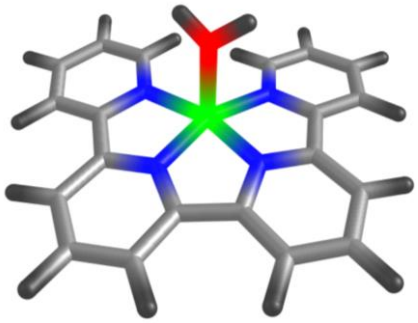

26	13.864050000	0.523580000	3.770666000
7	13.408197000	1.565840000	2.152622000
7	14.596863000	1.558893000	5.284191000
7	13.621467000	-0.905277000	2.568291000
7	14.302264000	-0.897242000	4.916824000
8	11.714558000	0.686509000	4.522424000
6	13.316184000	2.910657000	2.009667000
6	13.149270000	0.780957000	1.032174000
6	14.805355000	2.895739000	5.367504000
6	14.910463000	0.786929000	6.399475000
6	13.247037000	-0.642506000	1.280782000
6	13.779991000	-2.188406000	3.039785000
6	14.759308000	-0.633890000	6.178220000
6	14.200406000	-2.183788000	4.434647000
6	12.998132000	3.530073000	0.811825000
6	12.828715000	1.358158000	-0.202454000
6	15.268800000	3.523094000	6.512242000
6	15.372092000	1.374119000	7.584311000
6	13.014522000	-1.703653000	0.401426000
6	13.548835000	-3.264987000	2.195004000
6	15.068452000	-1.692271000	7.038343000
6	14.503981000	-3.256261000	5.260864000
6	12.754054000	2.738996000	-0.324373000

6	15.548054000	2.748878000	7.652457000
6	13.163593000	-3.015288000	0.864542000
6	14.927403000	-3.005089000	6.579527000
1	15.430397000	-1.492808000	8.046287000
1	15.168075000	-3.838849000	7.238072000
1	14.421104000	-4.276066000	4.886159000
1	15.595140000	0.739779000	8.441872000
1	15.905550000	3.216075000	8.569782000
1	15.406596000	4.603484000	6.510880000
1	14.588778000	3.473959000	4.471601000
1	13.484740000	3.502531000	2.907289000
1	12.934031000	4.616659000	0.773009000
1	12.503984000	3.197480000	-1.280777000
1	12.637652000	0.712281000	-1.059105000
1	12.723610000	-1.510140000	-0.630266000
1	12.982133000	-3.850987000	0.189524000
1	13.666546000	-4.284572000	2.560547000
1	11.678596000	0.986493000	5.450441000
1	11.223396000	1.364582000	4.020855000

Fe^{I} complex with 1 acetonitrile

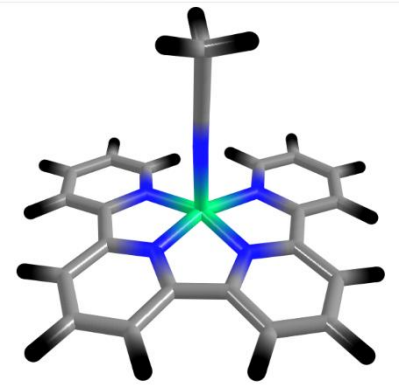

26	13.979101000	1.051458000	3.788416000
7	13.729228000	2.040348000	2.089019000
7	14.813351000	2.068896000	5.275911000
7	13.506956000	-0.390549000	2.663607000
7	14.390107000	-0.391281000	4.938393000
7	11.976833000	1.418887000	4.486429000
6	13.926798000	3.358283000	1.851898000
6	13.240869000	1.261867000	1.045376000
6	15.039640000	3.400346000	5.363388000
6	15.185521000	1.278672000	6.358115000
6	13.131651000	-0.142071000	1.372189000
6	13.590307000	-1.671251000	3.160168000

6	14.925007000	-0.132501000	6.169753000
6	14.101993000	-1.670319000	4.522158000
6	13.642937000	3.964887000	0.638721000
6	12.935124000	1.826405000	-0.199734000
6	15.616229000	4.005259000	6.469173000
6	15.774423000	1.839666000	7.498456000
6	12.757530000	-1.204286000	0.543639000
6	13.225802000	-2.748054000	2.363978000
6	15.168303000	-1.189343000	7.051397000
6	14.328084000	-2.741856000	5.374822000
6	13.129182000	3.183968000	-0.411553000
6	15.994418000	3.208423000	7.563895000
6	12.792493000	-2.507899000	1.047190000
6	14.861640000	-2.494411000	6.653114000
1	15.597600000	-0.996952000	8.033787000
1	15.045572000	-3.325735000	7.332736000
1	14.096801000	-3.756561000	5.052367000
1	16.054820000	1.190735000	8.327804000
1	16.449174000	3.654219000	8.448184000
1	15.758059000	5.085053000	6.474534000
1	14.722461000	4.001457000	4.513768000
1	14.324170000	3.943984000	2.677963000
1	13.818475000	5.033238000	0.521100000
1	12.891532000	3.632791000	-1.375739000
1	12.547616000	1.189383000	-0.994346000
1	12.457251000	-1.016910000	-0.486575000
1	12.504559000	-3.343722000	0.410642000
6	10.902195000	1.556241000	4.903270000
6	9.562596000	1.725073000	5.421927000
1	9.267310000	2.780505000	5.342386000
1	8.860026000	1.109607000	4.843441000
1	9.530309000	1.419554000	6.476840000
1	13.283928000	-3.762666000	2.756913000

Fe^{I} complex with square planar geometry

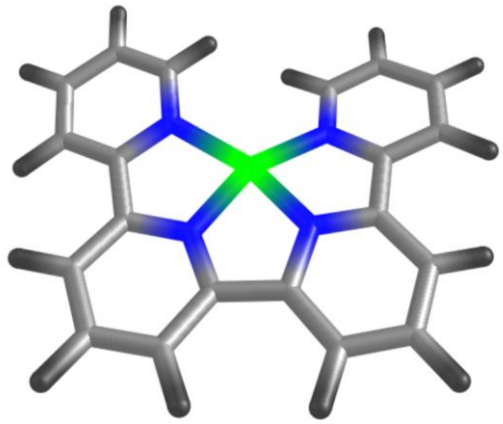

26	14.050524000	0.535232000	3.736356000
7	13.290199000	1.521523000	2.200089000
7	14.812818000	1.521208000	5.271770000
7	13.794637000	-0.922288000	2.549234000
7	14.308650000	-0.922363000	4.922878000
6	13.111166000	2.861164000	2.108682000
6	13.133492000	0.755499000	1.058368000
6	14.992245000	2.860823000	5.362912000
6	14.970055000	0.755306000	6.413537000
6	13.303684000	-0.669437000	1.295649000
6	13.852104000	-2.207618000	3.040893000
6	14.799765000	-0.669566000	6.176411000
6	14.251620000	-2.207640000	4.431016000
6	12.802513000	3.494822000	0.914167000
6	12.822105000	1.344774000	-0.169096000
6	15.301740000	3.494563000	6.557157000
6	15.282260000	1.344684000	7.640753000
6	12.963826000	-1.722707000	0.451574000
6	13.516074000	-3.286109000	2.222637000
6	15.140102000	-1.722849000	7.020298000
6	14.588133000	-3.286130000	5.249061000
6	12.658625000	2.724320000	-0.249112000
6	15.446099000	2.724193000	7.720471000
6	13.093185000	-3.041324000	0.913090000
6	15.011082000	-3.041425000	6.558615000
1	15.528567000	-1.521039000	8.017690000
1	15.279861000	-3.872770000	7.209156000
1	14.535427000	-4.301926000	4.858400000
1	15.386837000	0.719467000	8.526937000
1	15.687983000	3.195426000	8.672791000
1	15.441678000	4.574523000	6.569375000
1	14.902645000	3.423594000	4.434215000
1	13.200273000	3.424025000	3.037372000
1	12.662808000	4.574810000	0.901720000

1	12.417392000	3.195467000	-1.201638000
1	12.717913000	0.719459000	-1.055255000
1	12.575610000	-1.520883000	-0.545911000
1	12.824839000	-3.872656000	0.262353000
1	13.569150000	-4.301955000	2.613118000

References:

1. L. X. Chen and X. Zhang, *J.Phys.Chem.Lett.*, 2013, **4**, 4000-4013.
2. B. Ravel and M. Newville, *J.Synchrotron Radiat.*, 2005, **12**, 537-541.
3. G. Bunker, *Introduction to XAFS: A Practical Guide to X-ray Absorption Fine Structure Spectroscopy*, Cambridge University Press, Cambridge, 2010.
4. A. Iglesias-Juez, G. L. Chiarello, G. S. Patience and M. O. Guerrero-Pérez, *Can. J. Chem. Eng*. 2022, **100**, 3-22.
5. H. Husain, M. Sulthonul, B. Hariyanto, C. Cholsuk and S. Pratapa, *Mater. Today: Pro*, 2021, **44**, 3296-3300.
6. S. Calvin, *XAFS for Everyone*, CRC Press, Boca Raton. 2024.
7. F. Neese, *Wiley Interdiscip.Rev.Comput.Mol.Sci.*, 2012, **2**, 73-78.
8. P. J. Stephens, F. J. Devlin, C. F. Chabalowski and M. J. Frisch, *J.Phys.Chem.*, 1994, **98**, 11623-11627.
9. F. Weigend and R. Ahlrichs, *Phys.Chem.Chem.Phys.* 2005, **7**, 3297-3305.
10. S. Kossmann and F. Neese, *J.Chem. Theory. Comput.*, 2010, **6**, 2325-2338.
11. A. D. Becke, *J.Chem.Phys.*, 1993, **98**, 5648-5652.
12. S. Grimme, J. Antony, S. Ehrlich and H. Krieg, *J.Chem.Phys.*, 2010, **132**, 154104.
13. S. Grimme, S. Ehrlich and L. Goerigk, *J.Comput.Chem.*, 2011, **32**, 1456-1465.